Photoluminescent Properties of Carbon Nanodots

Bao-Ping Qi, Guo-Jun Zhang, Zhi-Ling Zhang and Dai-Wen Pang

Abstract With unique and tunable photoluminescent properties, carbon nanodots (CNDs), as a new class of optical tags, have been extensively studied. In this chapter, we introduce the basic knowledge with respect to CNDs, including their structures and compositions, optical properties and applications in the bioimaging and biosensors. In particular, the photoluminescence (PL) mechanisms of CNDs, which are able to instructively improve its optical properties, have been emphasized and discussed in details. We hope to inspire research into the origins of the unique properties of CNDs and intrigue the researchers with different research backgrounds to participate in this field and explore the PL mechanisms of CNDs.

Keywords Carbon nanodots · Photoluminescence · Mechanism · Density functional theory · Electrochemiluminescence

1 Introduction

Since carbon nanodots (CNDs) were accidentally discovered by Scrivens et al. in the process of purifying single-walled carbon nanotubes (SWCNTs) through arc-discharge methods [1], luminous CNDs have attracted a great deal of interests from the viewpoints of both fundamental studies and applications. Typically, CNDs are smaller than 10 nm in size, and show size- and excitation-dependent photoluminescence (PL) behaviors. CNDs are mainly composed of carbon, oxygen, and

B.-P. Qi · Z.-L. Zhang · D.-W. Pang (✉)
Key Laboratory of Analytical Chemistry for Biology and Medicine (Ministry of Education), College of Chemistry and Molecular Sciences, State Key Laboratory of Virology, The Institute for Advanced Studies, Wuhan Institute of Biotechnology, Wuhan University, Wuhan 430072, People's Republic of China
e-mail: dwpang@whu.edu.cn

G.-J. Zhang
School of Laboratory Medicine, Hubei University of Chinese Medicine, Huangjia Lake West Road, Wuhan 430065, People's Republic of China

N. Yang et al. (eds.), *Carbon Nanoparticles and Nanostructures*, Carbon Nanostructures, DOI 10.1007/978-3-319-28782-9_7

other heteroatom with many oxygenous functional groups at their surface [2, 3], thus imparting them with ease to be functionalized and excellent water solubility [4–6]. In addition, CNDs are characteristic of small sizes, low cytotoxicity, excellent photo-stability and chemical inertness [7]. Due to these features, CNDs have already displayed their potentials in biolabeling, in vivo, and dynamic tracer applications [8, 9].

One of the most notable issues is whether the emerging optical materials CNDs are able to displace the commonly used semiconductor quantum dots (QDs), having the unknown environmental and biological hazards for their heavy metal [10, 11]. The luminous carbonaceous CNDs exhibit low-toxicity and eco-friendly properties. However, compared with the QDs, the quantum yield of CNDs is much less, which would hinder their further developments and applications. Hence, it is necessary to make clear the PL mechanisms of CNDs to improve the quantum yield of CNDs. Both the complicated carbon/oxygen chemical bonds and the non-stoichiometric nature of CNDs make it difficult to study the intrinsic PL properties. Up to now, several PL mechanisms have been mainly suggested to originate from surface state, conjugated structures, special structure sites, etc. [12–15]. The viewpoint that the radiative recombinations of the CNDs surface-confined electrons and holes are responsible for the PL phenomenon is the surface state. The π-electron systems, zigzag sites and luminol-like units on the CNDs are also deemed to be the center of PL. The surface state is able to explain the excitation-dependent PL behaviors of CNDs, but the free zigzag sites are more suitable for the pH-dependent properties of CNDs. Up to now, none of them could account for all the PL phenomena of CNDs.

Herein, we introduce the CNDs regarding the structures and compositions, the basic optical properties and their applications in bioimaging and biosensors. In addition, we pay much attention to the PL mechanisms of CNDs, which is a significant aspect. We look forward to obtaining the better understanding into the origins of their PL behaviors, achieving higher quantum yield, and developing novel applications in further.

2 Structures and Compositions

CNDs are very small in size, and usually less than 10 nm (Fig. 1a). They are composed of a carbon backbone with sp^2 carbon or sp^3 carbon (Fig. 1c), and abundant in oxygen-containing groups at the edge or the base plane (Fig. 1b). The special structures of CNDs determine their special properties, among which the PL performance has caused widely public concern. Mostly, CNDs are divided into two members, carbon dots (CDs) and graphene quantum dots (GQDs). CDs are always spherical, and they are divided into carbon nanoparticles (CNPs) without crystal-lattice and carbon quantum dots (CQDs) with obvious crystal lattice. Another carbon-based nanomaterial, whose size and surface functionality are similar to the CDs, is GQDs. GODs have the lateral dimension larger than their height, which can be regarded as small pieces of graphene. The UV-visible absorptions and PL spectra

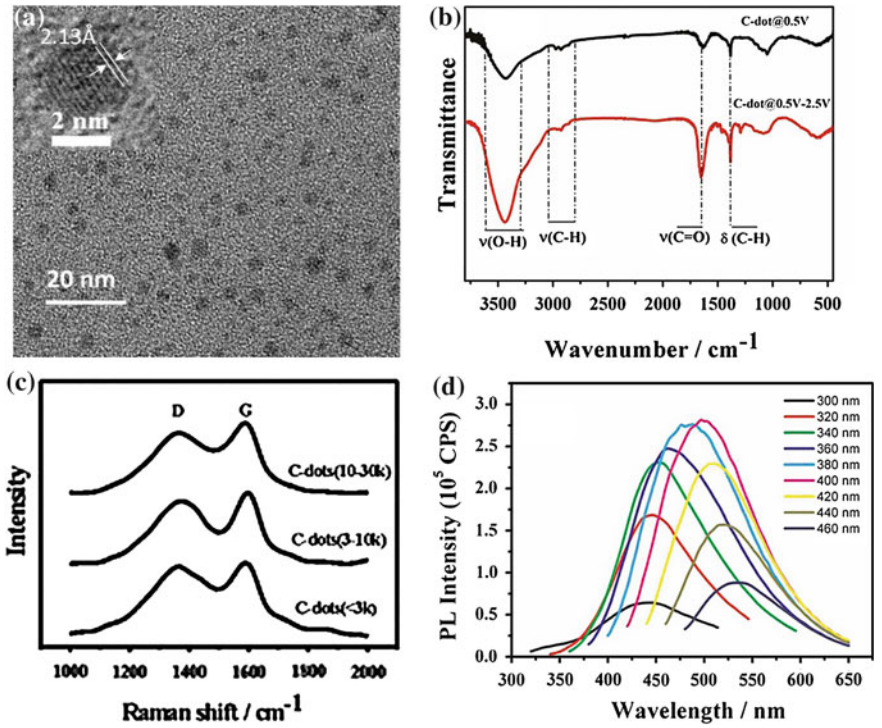

Fig. 1 **a** The high-resolution transmission electron microscopy images of CNDs [16]. **b** FT-IR spectra of CNDs [17]. **c** Raman spectra of CNDs [18]. **d** The excitation-dependent PL spectra of CNDs in water [17]

of the carbonaceous QDs (CQDs and GQDs) from the quantum confinement effect are not so clear, which are obviously different from those of the semiconductor QDs. So both GQDs and CQDs are not proper to be brought into the system of QDs. Typically, both CDs and GQDs display many parallel performances such as excitation-dependent PL behaviors (Fig. 1d). Based on these similar structures and properties, herein CDs and GQDs are also categorized as CNDs.

3 Optical Properties

3.1 Absorbance

CNDs typically show strong optical absorption in the UV region (200–320 nm) due to the effective photon-harvesting, with a tail extending out into the visible range.

Some CNDs exhibit two shoulder peaks in the strong background absorption, which are attributed to π-π* transition of C=C bonds and n-π* transition of C=O bonds, respectively (Fig. 2a).

3.2 Photoluminescence

From both fundamental and application-oriented stances, one of the most fascinating features of CNDs is their excitation dependence [7]. As compared with conventional organic dyes, the key advantage of CNDs include non-blinking PL and long-time photostability (Fig. 2c) [19]. It is exciting that their PL show tunable properties. Up to now, the CNDs with different PL colors, ranging from the visible region into the near-infrared region (Fig. 2b), have been fabricated by various methods [4, 18, 20].

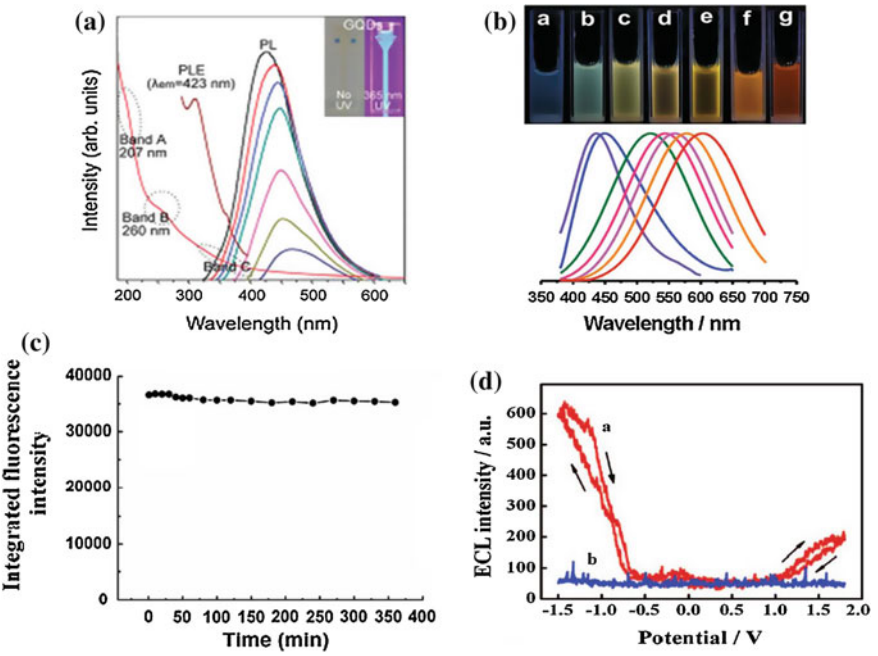

Fig. 2 **a** UV-visible absorption spectra of CNDs in water [35]. **b** *Top* Optical images of as-prepared multicolor fluorescent CNDs. *Bottom* PL spectra of CNDs [18]. **c** Dependence of fluorescence intensity on excitation time for CNDs in water [19]. **d** ECL responses: (*a*) with and (*b*) without CNDs at a Pt electrode in 0.1 M PBS (pH 7.0) [36]

3.3 Upconversion Photoluminescence

Upon simultaneous absorption of two or sequential absorption of multiple longer wavelength photons, the emission wavelength is shorter than the excitation wavelength, which is called upconversion PL. Some CNDs exhibit this PL feature [21–24]. Li et al. have reported that the CNDs prepared by the hydrazine hydrate reduction of graphene oxide with surface-passivated by a polyethylene glycol showed the upconverted emissions [25]. When the excitation wavelength changed from 600 to 800 nm, the upconverted emissions peaks shifted from 390 to 468 nm, respectively. The shifting between the energy of the upconverted emission wavelength and the excitation wavelength was almost unchanged and stayed around 1.1 eV, which was close to the δE between the σ and π orbitals. Based on this conclusion, they speculate on the upconversion PL due to the anti-Stokes PL. Since the long excitation wavelength owns the traits of deep-tissue penetration, low photon-induced toxicity, low back ground interference, etc., upconversion PL will enable CNDs to be desirable materials in in vivo imaging.

3.4 Electrochemiluminescence (ECL)

Similar to QDs [26, 27] and Si nanodots [28], CNDs exhibit ECL properties as well. For the first time, Chi et al. have reported the ECL phenomenon of the CNDs solution at a Pt disk working electrode (Fig. 2d). The ECL mechanism of the CNDs was suggested to involve the formation of excited-state CNDs (R*) via electron-transfer annihilation of negatively charged ($R^{\cdot -}$) and positively charged ($R^{\cdot +}$) CNDs. The intensity of cathodic ECL was larger than that of anodic ECL, indicating that $R^{\cdot +}$ was more stable than $R^{\cdot -}$. From then on, the ECL properties of CNDs have progressively drawn attention [29–32].

ECL was demonstrated to be more sensitive than PL to surface chemistry, which makes it a powerful tool to study surface states of nanocrystals [33]. Especially, the current signal and the light signal are obtained simultaneously, facilitating the investigation of light emission mechanism of the luminophor [34]. It is of great significance to compare the ECL spectrum with PL spectrum of CNDs, which will be discussed in the following.

4 Photoluminescence Mechanisms

Although CNDs have been studied for ten years, knowledge into the origins of their PL is still an open question and requires further clarification. The PL phenomena of CNDs have been mainly suggested to originate from surface state, conjugated structures, special structure sites, etc. On one hand, the quantum yields of CNDs are

lower than those of QDs. On the other hand, the CNDs prepared by various methods from different raw materials are mainly blue or green in color. In order to effectively improve the optical properties of CNDs, a generally recognized PL mechanism capable of explaining all the PL phenomena of CNDs is urgently needed.

4.1 Surface State

The periodic lattices in the crystals are destroyed in some directions, resulting in a new state near the surface, which is the so-called surface state. The surface state in CNDs has been deemed to be the hybridization of the carbon backbone and the linked functional groups [12]. The characteristics of the excitation dependence from CNDs may reflect that there is a distribution of different emissive sites in each CNDs [7]. Sun et al. have attributed the PL from CNDs to the presence of surface energy traps that became emissive upon stabilization as a result of the surface passivation. The electrons and holes were generated likely by efficient photoinduced charge separations in the CNDs, and the roles of surface passivation by the organic or other functionalization was able to make the surface sites more stable to facilitate more effective radiative recombinations. At the same time, they draw a conclusion that there must be a quantum confinement of emissive energy traps to the particle surface, since the larger CNDs with the same surface passivation were found to be much less luminescent [15].

The CNDs prepared by different kinds of methods also exhibited the behaviors of excitation dependence [37–40], but no additional passivation step was required for PL to occur. In common, there are more or less oxygenous functional groups on the surface of CNDs. The oxygen-based groups on the carbon core could be regarded as the primary surface state of CNDs. From then on, lots of researches have been focused on the effect of oxygenous groups on the PL of CNDs. Zheng et al. [41] have reported that the CNDs with green emission could be changed to the blue ones through $NaBH_4$ reduction. Liu et al. [42] have prepared blue-color emissions of CNDs without oxygenous defects and their oxidized form with green-color emissions. They reveal that the green PL of CNDs originates from defect states with oxygenous functional groups, whereas the blue luminescence of CNDs is dominated by intrinsic states in the high-crystalline structure.

Our group has investigated the surface oxidation degree on the PL of CNDs in detail and proposed a surface oxidation-related PL mechanism for CNDs [17, 18, 43]. Bao et al. [17] have developed an electrochemical method to prepare luminescent CNDs with controllable sizes. The higher the applied potentials, the smaller the resulting CNDs. Importantly, once the CNDs were exfoliated into the solution, the size of the as-prepared CNDs would not change further, making it possible for the further electrochemical oxidation. The as-prepared CNDs at 0.5 V were further electrochemically oxidized at a home-made platinum cup electrode at 2.5 V. After that, the optimal emission wavelength of the further oxidized CNDs was red-shifted

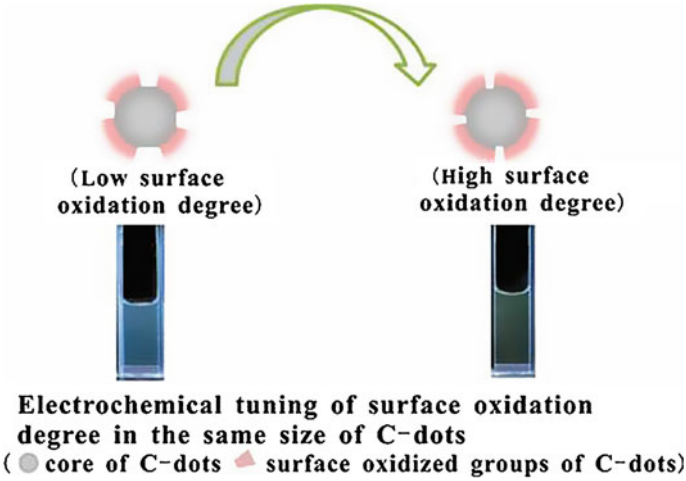

Fig. 3 Illustration of emission from CNDs along with the variation of surface oxidation degree [17]

by ca. 45 nm. In other words, the high surface oxidation degree resulted in the red-shifted PL of CNDs (Fig. 3). Surface states are the key to the PL of the CNDs. This work opens a new window not only to controllably prepare CNDs with small sizes and long emission wavelengths, but also to understand the PL mechanisms of CNDs. Our group [43] has also obtained two kinds of CNDs with the shifting or non-shifting PL at varied excitations by electro-oxidizing carbon paste electrodes with different compositions. CNDs with more complex surface states, related to a higher degree of surface oxidation, afford fluorescence emissions with varied energies at different excitations. However, it is demonstrated that CNDs with less surface states have the non-shifting fluorescence properties. Therefore, the emissions are proposed to be mainly attributed to the surface states caused by the surface oxidation of CNDs.

In order to confirm the surface state on the surface of CNDs, ECL, which is a highly sensitive technique for probing the surface of nanoparticles [44], has been adopted to probe the surface-state electronic transitions of the CNDs. Most ECL phenomena from semiconductor QDs have been observed to originate from surface states, which are often significantly red shifted from the PL peaks by as much as hundreds of nanometers, since these defect states are located in the band gap [27, 44, 45]. Ding et al. have discovered that the ECL spectrum of CNDs prepared by electrochemical etching was red shifted about 50 nm from the PL spectrum in organic solution [30]. The authors attributed the origin of both the ECL and PL to the surface traps in CNDs. Dong et al. [46] have obtained a series of the oxidized CNDs with the same oxidation degree by chemical oxidation. The PL spectra of the oxidized CNDs with different sizes (1–3, 3–5, 5–10, 10–30 kDa) were particle sized-dependent, but interestingly, ECL spectra of CNDs were all 600 nm, showing

size-independent. It indicates that ECL of CNDs is dependent on the presence of surface states rather than size of particles. Our group has also obtained CNDs with different sizes (<3 k, 3–10 k, 10–30 kDa) by ultrafiltration separation and each ECL peak was very close to its corresponding PL peak, indicating that the PL of CNDs most likely emit from the same surface emissive sites as the ECL of the CNDs [18].

These studies show the ECL spectra of CNDs are tinily red-shifted compared with those of QDs. In addition, the broad emission spectra of CNDs make them hard to distinguish between the PL and ECL spectra. The relationship between ECL phenomena and the surface traps of CNDs is still poorly understood, and the better materials are anticipated.

4.2 Conjugate Structures

The sp^2 domain CNDs with hardly oxygenous defects, achieved by both physical exfoliation of graphite nanoparticles and intercalation into graphite through special compounds, show PL properties [42, 47]. Some studies have demonstrated the possibility of tailoring the sp^2 domains and designing the edge structures of CNDs. Li et al. have achieved the full sp^2 domain CNDs with different sizes through chemical synthesis, clearly demonstrating that a large sp^2 domain results in the decrease of band gap [48–51]. However, the complex synthetic steps and the strong tendency to aggregate hinder its future development. By electrooxidation of graphite, our group has obtained two kinds of CNDs with blue and yellow emissions, respectively [19]. The red shift in the emission wavelength was attributed to the increase of the conjugation system, which was testified by the peak position of ν(C=O) in FTIR.

The density functional theory (DFT) has been widely used in the study of CNDs with single layer, which can provide a convincing evidence for the conjugated structures-related PL mechanism. Theoretical modelling and calculations allow precise isolation of the influence of each factor while fixing the others. Eda et al. [52] have reported that sp^2 domains isolated within sp^3 carbon matrix were responsible for the observed blue fluorescence from graphene oxide, which was firstly supported by calculations based on DFT. To confirm that the strong emission comes from the quantum-sized graphite fragment of CNDs, Li et al. [53] have performed theoretical calculations to investigate the relationship between luminescence and cluster sizes. As the size of the fragment increases, the gap decreases gradually, which is in good agreement with Eda's report. In order to study the effect of conjugated structures on PL properties of CNDs, our group has developed an efficient strategy edge-functionalization method [16]. The added conjugated structures through the formation of aromatic pyrazine led to the red-shifted emissions of CNDs, which was testified by DFT-based calculation (Fig. 4). Both the experimental results and the DFT-based calculations suggest that the mechanism for conjugated structures in CNDs to tune the band gap of CNDs. Sk et al. [54] have

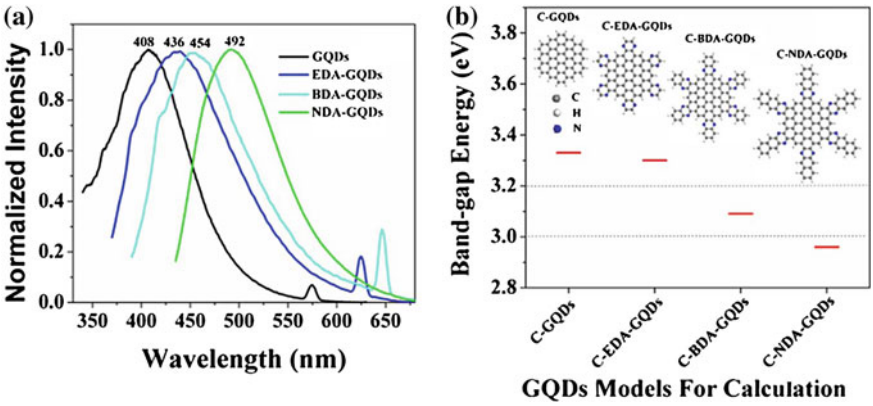

Fig. 4 **a** The PL emission spectra of CNDs dispersed in ethanol. **b** The calculated band-gap energy of the corresponding CNDs dispersed in ethanol based on DFT. The *inset* shows the structures of CNDs used for calculations [16]

revealed that the PL of CNDs is sensitively affected by their size and covers the entire visible light spectrum by varying the size of sp^2 domains from 0.89 to 1.80 nm based on the DFT and time-dependent DFT calculations.

4.3 Special Structure Sites

Owing to the small diameter of CNDs, Pan et al. have proposed that there is a high concentration of free zigzag sites at the edge of CNDs, leading to the strong PL [55]. It may originate from free zigzag sites with a carbene-like triplet ground state (Fig. 5). The energy difference (δE) between the two electronic transitions observed in the PL emission of CNDs is determined to be 0.96 eV, within the value (<1.5 eV) for triple carbenes defined by Hoffmann. The proposed PL mechanism based on the emissive free zigzag sites could explain pH-dependent PL phenomena of CNDs. Under acidic conditions, the free zigzag sites of CNDs are protonated, forming a reversible complex between the zigzag sites and H^+. Thus the emissive triple carbene state is broken and becomes inactive in PL. However, under alkaline conditions, the free zigzag sites are restored, thereby leading to the restoration of PL. If pH is switched repeatedly between 13 and 1, the PL intensity varies reversibly.

The main PL spectrum, chemiluminescence (CL) spectrum and ECL spectrum of hydrazide-modified CNDs are essentially the same, implying that the three spectra are given by similar excited states [56]. It has also been reported that refluxing CNDs with N_2H_4 would result in the formation of abundant luminol-like units at the edges of CNDs, which is a well-known luminophore, exhibiting excellent PL, CL and ECL properties. The main PL spectrum of hydrazide-modified CNDs is quite

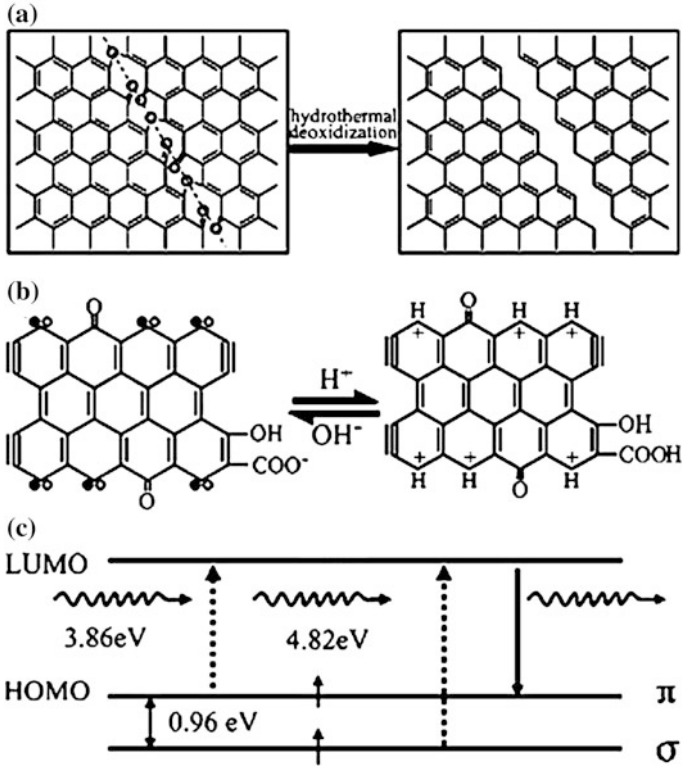

Fig. 5 **a** Mechanism for the preparation of CNDs. **b** Models of the CNDs in acidic and alkali media. The two models can be converted reversibly depending on pH. The pairing of σ(•) and π(o) localized electrons at carbene-like zigzag sites and the presence of triple bonds at the carbyne-like armchair sites are represented. **c** Typical electronic transitions of triple carbenes at zigzag sites [55]

similar to that of luminol, suggesting that the PL of CNDs might be derived from the luminol-like units.

PL mechanisms of CNDs may be attributed to either combining effect or competition between the intrinsic and defect state emission. Our group has revealed that the PL properties of CNDs were mainly influenced by both their size and degree of surface oxidation through surface analytical techniques time-resolved photoluminescence spectroscopy and the ECL technique [18]. Increasing the degree of surface oxidation leads to a narrowing of the energy gap of the surface; meanwhile, larger CNDs with an extensive π-electron system, which couple with surface electronic states, can also lead to a narrowing of the energy gap of the surface states. Sun et al. have classified the emissions of CNDs into two primary categories: emissions that originate from created or induced energy band gaps in a single graphene sheet and emissions that are associated with defects in single- and/or multiple-layer graphene [13]. They have proposed that the band gap fluorescence in

graphene is associated with the conjugated structures on a single sheet, which is quenched by π-domains in neighboring sheets in a few-layer configuration. However, the defect-derived emissions are associated with the defect site across several sheets in a similar few-layer configuration, and thus little affected by the interlayer interactions.

Though the above PL mechanisms have been raised, none of them is able to explain all the PL phenomena of CNDs. Obviously, PL mechanism of CNDs is currently ambiguous. To resolve it, researchers in different fields are needed to participate in this study.

5 Applications

5.1 Bioimaging

The luminous CNDs combined with the characteristics of excellent photostability, ease to be functionalized, low cytotoxicity, chemical inertness, and small size, render them applicable in bioimaging, biolabeling and dynamic tracer [8]. Our group has reported that the multicolor CNDs showed low cytotoxicity to the VERO cells through 3-(4,5-dimethylthiazol-2-yl)-2,5-diphenyltetrazolium bromide (MTT) and finally realized the multicolor imaging of cells [18]. The cells efficiently took up CNDs, which was regarded as an endocytosis mechanism [57–59]. Lee et al. have first studied the in vivo bio-distribution and the potential toxicity of CNDs (Fig. 6) [60]. Four kinds of cancer cells and one kind of normal cell were chosen as in vitro cell culture models to examine the possible adverse effects of CNDs. At the tested exposure levels, no acute toxicity or morphological changes were noted in KB, MDA-MB231, A549 cancer cells, and MDCK normal cells, respectively. A long-term in vivo study revealed that CNDs mainly accumulated in liver, spleen, lung, kidney, and tumor sites after intravenous injection. The serum biochemical analysis and histological evaluation study revealed that CNDs did not cause appreciable toxicity to the treated mice. With adequate studies of toxicity, both in vitro and in vivo, luminous CNDs may be considered for potential biological applications. Chen et al., have demonstrated that CNDs could be used to specifically label and track molecular targets involved in dynamic cellular processes in live cells [61]. The internalization, trafficking, and recycling of insulin receptors in adipocytes have been monitored in real-time by using insulin-conjugated CNDs, which were synthesized through amidation reaction. They reveal for the first time that the insulin receptor dynamics are stimulated by apelin and inhibited by TNFα, providing evidence for the molecular mechanisms underlying the regulation of these cytokines in insulin sensitivity. These activities have been successfully proceeded, which can be attributed to the excellent photostability of CNDs. This study demonstrates the great potentials of CNDs in live-cell imaging, particularly for investigating dynamic cellular processes.

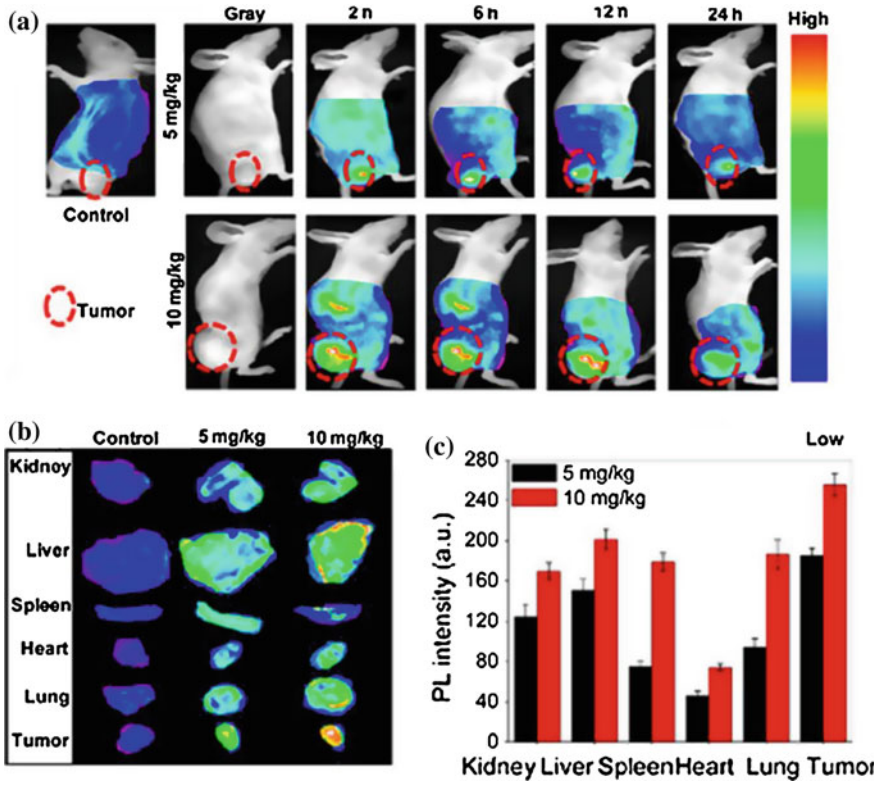

Fig. 6 In vivo imaging and biodistribution of CNDs. **a** The in vivo imaging of KB tumor bearing mice after intravenous injection of CNDs, **b** ex vivo images of isolated organs of mice at 24 h after injection of CNDs, and **c** PL intensities of the carboxylated CNDs from isolated organs at different dosages [60]

5.2 Sensors

Based on PL and ECL properties of CNDs discussed above, various sensors have been designed as signal-off or signal-on processes to detect the target. Zhao et al. have provided a novel and versatile signaling transduction strategy in the fluoroimmunoassay through regulating the interaction between graphene and CNDs (Fig. 7) [62]. When adding graphene to the mIgG-CNDs solution, the π-π stacking interaction between graphene and CNDs could bring graphene and CNDs into resonance energy transfer (RET) proximity to facilitate the PL quenching of CNDs. In the sensing process, the addition of IgG specifically linked with the mIgG increases the distance between CNDs and graphene surface, resulting in restoration the PL of CNDs. Based on fluorescence resonance energy transfer (FRET) from upconverting phosphors (UCPs) to CNDs, our group has also presented a new aptamer biosensor for thrombin [63].

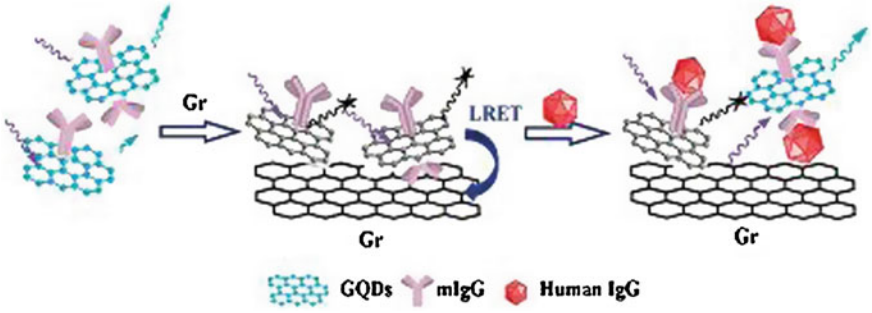

Fig. 7 Schematic illustration of a universal immunosensing strategy based on regulation of the interaction between graphene and CNDs [62]

Since Chi et al. have reported that CNDs can generate the ECL signal, CNDs has been widely used in the fabrication of the ECL-related sensors [64–71]. Zhu et al. have reported that the co-reaction reagent $S_2O_8^{2-}$ could significantly increase the ECL signal of the CNDs [31], and a novel ECL sensor for Cd^{2+} has been proposed based on the competitive coordination between the chelator cysteine and CNDs for metal ions. For the first time, our group has demonstrated that CNDs prepared by electrochemical etching could act as the coreactants for the anodic ECL of $Ru(bpy)_3^{2+}$ [72]. It has been suggested that the benzylic alcohol units on the CNDs are responsible for the capability as core actants in the anodic ECL process of $Ru(bpy)_3^{2+}$/CNDs. For the low biotoxicity, the system $Ru(bpy)_3^{2+}$/CNDs would be much promising in bioanalysis, which was exemplified by the quantitative detection of dopamine molecules. This work has deepened and broadened the knowledge of CNDs.

In addition, CNDs has also been applied in the fields of photocatalyst [53], organic photovoltaic (OPV) devices [73], oxygen reduction reaction [49, 74], etc. Due to the special structures, CNDs shows the peroxidase-like activities, realizing the great performance and stability in H_2O_2 detection [75, 76].

6 In Conclusion

Based on the excellent photostability, ease to be functionalized, low cytotoxicity, and chemical inertness, the luminous CNDs with small sizes have, no doubt, brought about tremendous interest. They would have the potentials to partially take the place of QDs. However, the research on CNDs is still in its early stage, and the PL from most CNDs with low quantum yields is blue or green. It is particularly important that the explicit PL mechanism of CNDs will facilitate the improvement of the quantum yields and the red-shifted emission.

Obviously, the ambiguous PL mechanism of CNDs hindered their developments. Herein, we would like to share our viewpoints on some critical issues on the PL mechanism of CNDs. On one hand, it is necessary to make clear the effect of the

oxygenous functional groups on the surface of CNDs on the PL properties of CNDs. The present CNDs contain the comparatively high oxygen content and different kinds of the oxygenous groups result in their structure complexities. But, the effect of each oxygenous group on the PL properties of CNDs is not uncertain. The DFT-based calculations should be employed to study these problems in details via designing the reasonable theoretical models. On the other hand, the better fabrication and separation methods for the CNDs are of great importance. The PL of CNDs with the narrow peak width will provide more accurate information in comparison with the spectrum of ECL. At the same time, the more appropriate materials, such as a series of CNDs with different sizes but the same surface, are in urgent need for the ECL technique. For the complexity of the CNDs, more methods and more researchers in different fields are anticipated to participate in this domain.

CNDs have shown primary potential in imaging and related biosensor applications. Once the low toxic CNDs possess high quantum yield and tunable PL, they will have a huge impact in both health and environmental applications.

Acknowledgments This work was supported by the National Basic Research Program of China (973 Program, Grant No. 2011CB933600), the National Natural Science Foundation of China (Grant No. 21535005), the 111 Project (111-2-10), and Collaborative Innovation Center for Chemistry and Molecular Medicine.

References

1. X. Xu, R. Ray, Y. Gu, H.J. Ploehn, L. Gearheart, K. Raker, W.A. Scrivens, Electrophoretic analysis and purification of fluorescent single-walled carbon nanotube fragments. J. Am. Chem. Soc. **126**(40), 12736–12737 (2004). doi:10.1021/ja040082h
2. W. Kwon, J. Lim, J. Lee, T. Park, S.-W. Rhee, Sulfur-incorporated carbon quantum dots with a strong long-wavelength absorption band. J. Mater. Chem. C **1**(10), 2002–2008 (2013). doi:10.1039/c3tc00683b
3. Y.P. Sun, X. Wang, F.S. Lu, L. Cao, M.J. Meziani, P.J.G. Luo, L.R. Gu, L.M. Veca, Doped carbon nanoparticles as a new platform for highly photoluminescent dots. J. Phys. Chem. C **112**(47), 18295–18298 (2008). doi:10.1021/jp8076485
4. H. Tetsuka, R. Asahi, A. Nagoya, K. Okamoto, I. Tajima, R. Ohta, A. Okamoto, Optically tunable amino-functionalized graphene quantum dots. Adv. Mater. **24**(39), 5333–5338 (2012). doi:10.1002/adma.201201930
5. F. Jiang, D. Chen, R. Li, Y. Wang, G. Zhang, S. Li, J. Zheng, N. Huang, Y. Gu, C. Wang, C. Shu, Eco-friendly synthesis of size-controllable amine-functionalized graphene quantum dots with antimycoplasma properties. Nanoscale **5**(3), 1137–1142 (2013). doi:10.1039/c2nr33191h
6. S.J. Zhu, Q.N. Meng, L. Wang, J.H. Zhang, Y.B. Song, H. Jin, K. Zhang, H.C. Sun, H.Y. Wang, B. Yang, Highly photoluminescent carbon dots for multicolor patterning, sensors, and bioimaging. Angew. Chem. Int. Ed. **52**(14), 3953–3957 (2013). doi:10.1002/anie.201300519
7. S.N. Baker, G.A. Baker, Luminescent carbon nanodots: emergent nanolights. Angew. Chem. Int. Ed. **49**(38), 6726–6744 (2010). doi:10.1002/anie.200906623
8. C.Q. Ding, A.W. Zhu, Y. Tian, Functional surface engineering of C-dots for fluorescent biosensing and in vivo bioimaging. Acc. Chem. Res. **47**(1), 20–30 (2014). doi:10.1021/ar400023s

9. J. Shen, Y. Zhu, X. Yang, C. Li, Graphene quantum dots: emergent nanolights for bioimaging, sensors, catalysis and photovoltaic devices. Chem. Commun. **48**(31), 3686–3699 (2012). doi:10.1039/c2cc00110a
10. Y.Y. Su, Y. He, H.T. Lu, L.M. Sai, Q.N. Li, W.X. Li, L.H. Wang, P.P. Shen, Q. Huang, C.H. Fan, The cytotoxicity of cadmium based, aqueous phase-synthesized, quantum dots and its modulation by surface coating. Biomaterials **30**(1), 19–25 (2009). doi:10.1016/j.biomaterials.2008.09.029
11. Y.Y. Su, M. Hu, C.H. Fan, Y. He, Q.N. Li, W.X. Li, L.H. Wang, P.P. Shen, Q. Huang, The cytotoxicity of CdTe quantum dots and the relative contributions from released cadmium ions and nanoparticle properties. Biomaterials **31**(18), 4829–4834 (2010). doi:10.1016/j.biomaterials.2010.02.074
12. S. Zhu, Y. Song, X. Zhao, J. Shao, J. Zhang, B. Yang, The photoluminescence mechanism in carbon dots (graphene quantum dots, carbon nanodots, and polymer dots): current state and future perspective. Nano Res. **8**(2), 355–381 (2015). doi:10.1007/s12274-014-0644-3
13. L. Cao, M.J. Meziani, S. Sahu, Y.P. Sun, Photoluminescence properties of graphene versus other carbon nanomaterials. Acc. Chem. Res. **46**(1), 171–180 (2013). doi:10.1021/ar300128j
14. L. Li, G. Wu, G. Yang, J. Peng, J. Zhao, J.-J. Zhu, Focusing on luminescent graphene quantum dots: current status and future perspectives. Nanoscale **5**(10), 4015–4039 (2013). doi:10.1039/c3nr33849e
15. Y.P. Sun, B. Zhou, Y. Lin, W. Wang, K.A. Fernando, P. Pathak, M.J. Meziani, B.A. Harruff, X. Wang, H. Wang, P.G. Luo, H. Yang, M.E. Kose, B. Chen, L.M. Veca, S.Y. Xie, Quantum-sized carbon dots for bright and colorful photoluminescence. J. Am. Chem. Soc. **128**(24), 7756–7757 (2006). doi:10.1021/ja062677d
16. B.P. Qi, H. Hu, L. Bao, Z.L. Zhang, B. Tang, Y. Peng, B.S. Wang, D.W. Pang, An efficient edge-functionalization method to tune the photoluminescence of graphene quantum dots. Nanoscale **7**(14), 5969–5973 (2015). doi:10.1039/C5nr00842e
17. L. Bao, Z.L. Zhang, Z.Q. Tian, L. Zhang, C. Liu, Y. Lin, B. Qi, D.W. Pang, Electrochemical tuning of luminescent carbon nanodots: from preparation to luminescence mechanism. Adv. Mater. **23**(48), 5801–5806 (2011). doi:10.1002/adma.201102866
18. L. Bao, C. Liu, Z.L. Zhang, D.W. Pang, Photoluminescence-tunable carbon nanodots: surface-state energy-gap tuning. Adv. Mater. **27**(10), 1663–1667 (2015). doi:10.1002/adma.201405070
19. Q.L. Zhao, Z.L. Zhang, B.H. Huang, J. Peng, M. Zhang, D.W. Pang, Facile preparation of low cytotoxicity fluorescent carbon nanocrystals by electrooxidation of graphite. Chem. Commun. **41**, 5116–5118 (2008). doi:10.1039/b812420e
20. X.M. Li, S.P. Lau, L.B. Tang, R.B. Ji, P.Z. Yang, Multicolour light emission from chlorine-doped graphene quantum dots. J. Mater. Chem. C **1**(44), 7308–7313 (2013). doi:10.1039/c3tc31473a
21. M. Li, W. Wu, W. Ren, H.-M. Cheng, N. Tang, W. Zhong, Y. Du, Synthesis and upconversion luminescence of N-doped graphene quantum dots. Appl. Phys. Lett. **101**(10), 103107 (2012). doi:10.1063/1.4750065
22. A. Salinas-Castillo, M. Ariza-Avidad, C. Pritz, M. Camprubi-Robles, B. Fernandez, M. J. Ruedas-Rama, A. Megia-Fernandez, A. Lapresta-Fernandez, F. Santoyo-Gonzalez, A. Schrott-Fischer, L.F. Capitan-Vallvey, Carbon dots for copper detection with down and upconversion fluorescent properties as excitation sources. Chem. Commun. **49**(11), 1103–1105 (2013). doi:10.1039/c2cc36450f
23. C. Wang, X. Wu, X. Li, W. Wang, L. Wang, M. Gu, Q. Li, Upconversion fluorescent carbon nanodots enriched with nitrogen for light harvesting. J. Mater. Chem. **22**(31), 15522 (2012). doi:10.1039/c2jm30935a
24. X.M. Wen, P. Yu, Y.R. Toh, X.Q. Ma, J. Tang, On the upconversion fluorescence in carbon nanodots and graphene quantum dots. Chem. Commun. **50**(36), 4703–4706 (2014). doi:10.1039/C4cc01213e

25. J. Shen, Y. Zhu, C. Chen, X. Yang, C. Li, Facile preparation and upconversion luminescence of graphene quantum dots. Chem. Commun. **47**(9), 2580–2582 (2011). doi:10.1039/c0cc04812g
26. L. Bao, L. Sun, Z.-L. Zhang, P. Jiang, F.W. Wise, H.D. Abruña, D.-W. Pang, Energy-level-related response of cathodic electrogenerated-chemiluminescence of self-assembled CdSe/ZnS quantum dot films. J. Phys. Chem. C **115**(38), 18822–18828 (2011). doi:10.1021/jp205419z
27. L. Sun, L. Bao, B.R. Hyun, A.C. Bartnik, Y.W. Zhong, J.C. Reed, D.W. Pang, H.D. Abruna, G.G. Malliaras, F.W. Wise, Electrogenerated chemiluminescence from PbS quantum dots. Nano Lett. **9**(2), 789–793 (2009). doi:10.1021/nl803459b
28. Z. Ding, B.M. Quinn, S.K. Haram, L.E. Pell, B.A. Korgel, A.J. Bard, Electrochemistry and electrogenerated chemiluminescence from silicon nanocrystal quantum dots. Science **296** (5571), 1293–1297 (2002). doi:10.1126/science.1069336
29. H. Zhu, X. Wang, Y. Li, Z. Wang, F. Yang, X. Yang, Microwave synthesis of fluorescent carbon nanoparticles with electrochemiluminescence properties. Chem. Commun. **34**, 5118–5120 (2009). doi:10.1039/b907612c
30. J. Zhou, C. Booker, R. Li, X. Sun, T.-K. Sham, Z. Ding, Electrochemistry and electrochemiluminescence study of blue luminescent carbon nanocrystals. Chem. Phys. Lett. **493**(4–6), 296–298 (2010). doi:10.1016/j.cplett.2010.05.030
31. L.-L. Li, J. Ji, R. Fei, C.-Z. Wang, Q. Lu, J.-R. Zhang, L.-P. Jiang, J.-J. Zhu, A facile microwave avenue to electrochemiluminescent two-color graphene quantum dots. Adv. Funct. Mater. **22**(14), 2971–2979 (2012). doi:10.1002/adfm.201200166
32. J. Lu, M. Yan, L. Ge, S. Ge, S. Wang, J. Yan, J. Yu, Electrochemiluminescence of blue-luminescent graphene quantum dots and its application in ultrasensitive aptasensor for adenosine triphosphate detection. Biosens. Bioelectron. **47**, 271–277 (2013). doi:10.1016/j.bios.2013.03.039
33. M.M. Richter, Electrochemiluminescence (ECL). Chem. Rev. **104**(6), 3003–3036 (2004). doi:10.1021/cr020373d
34. L. Hu, G. Xu, Applications and trends in electrochemiluminescence. Chem. Soc. Rev. **39**(8), 3275–3304 (2010). doi:10.1039/b923679c
35. L. Lin, S. Zhang, Creating high yield water soluble luminescent graphene quantum dots via exfoliating and disintegrating carbon nanotubes and graphite flakes. Chem. Commun. **48**(82), 10177–10179 (2012). doi:10.1039/C2CC35559K
36. L. Zheng, Y. Chi, Y. Dong, J. Lin, B. Wang, Electrochemiluminescence of water-soluble carbon nanocrystals released electrochemically from graphite. J. Am. Chem. Soc. **131**(13), 4564–4565 (2009). doi:10.1021/ja809073f
37. K. Jiang, S. Sun, L. Zhang, Y. Lu, A. Wu, C. Cai, H. Lin, Red, Green, and blue luminescence by carbon dots: full-color emission tuning and multicolor cellular imaging. Angew. Chem. Int. Ed. **54**(18), 5360–5363 (2015). doi:10.1002/anie.201501193
38. M.J. Krysmann, A. Kelarakis, P. Dallas, E.P. Giannelis, Formation mechanism of carbogenic nanoparticles with dual photoluminescence emission. J. Am. Chem. Soc. **134**(2), 747–750 (2012). doi:10.1021/ja204661r
39. J. Zhou, C. Booker, R. Li, X. Zhou, T.K. Sham, X. Sun, Z. Ding, An electrochemical avenue to blue luminescent nanocrystals from multiwalled carbon nanotubes (MWCNTs). J. Am. Chem. Soc. **129**(4), 744–745 (2007). doi:10.1021/ja0669070
40. C.S. Lim, K. Hola, A. Ambrosi, R. Zboril, M. Pumera, Graphene and carbon quantum dots electrochemistry. Electrochem. Commun. **52**, 75–79 (2015). doi:10.1016/j.elecom.2015.01.023
41. H. Zheng, Q. Wang, Y. Long, H. Zhang, X. Huang, R. Zhu, Enhancing the luminescence of carbon dots with a reduction pathway. Chem. Commun. **47**(38), 10650–10652 (2011). doi:10.1039/c1cc14741b
42. F. Liu, M.H. Jang, H.D. Ha, J.H. Kim, Y.H. Cho, T.S. Seo, Facile synthetic method for pristine graphene quantum dots and graphene oxide quantum dots: origin of blue and green luminescence. Adv. Mater. **25**(27), 3657–3662 (2013). doi:10.1002/adma.201300233

43. Y.-M. Long, C.-H. Zhou, Z.-L. Zhang, Z.-Q. Tian, L. Bao, Y. Lin, D.-W. Pang, Shifting and non-shifting fluorescence emitted by carbon nanodots. J. Mater. Chem. **22**(13), 5917–5920 (2012). doi:10.1039/c2jm30639e
44. N. Myung, Z.F. Ding, A.J. Bard, Electrogenerated chemiluminescence of CdSe nanocrystals. Nano Lett. **2**(11), 1315–1319 (2002). doi:10.1021/nl0257824
45. N. Myung, Y. Bae, A.J. Bard, Effect of surface passivation on the electrogenerated chemiluminescence of CdSe/ZnSe nanocrystals. Nano Lett. **3**(8), 1053–1055 (2003). doi:10.1021/nl034354a
46. Y. Dong, N. Zhou, X. Lin, J. Lin, Y. Chi, G. Chen, Extraction of electrochemiluminescent oxidized carbon quantum dots from activated carbon. Chem. Mater. **22**(21), 5895–5899 (2010). doi:10.1021/cm1018844
47. S.H. Song, M.H. Jang, J. Chung, S.H. Jin, B.H. Kim, S.H. Hur, S. Yoo, Y.H. Cho, S. Jeon, Highly efficient light-emitting diode of graphene quantum dots fabricated from graphite intercalation compounds. Adv. Opt. Mater. **2**(11), 1016–1023 (2014). doi:10.1002/adom.201400184
48. X. Yan, B. Li, L.S. Li, Colloidal graphene quantum dots with well-defined structures. Acc. Chem. Res. **46**(10), 2254–2262 (2013). doi:10.1021/ar300137p
49. Q. Li, S. Zhang, L. Dai, L.S. Li, Nitrogen-doped colloidal graphene quantum dots and their size-dependent electrocatalytic activity for the oxygen reduction reaction. J. Am. Chem. Soc. **134**(46), 18932–18935 (2012). doi:10.1021/ja309270h
50. X. Yan, X. Cui, L.S. Li, Synthesis of large, stable colloidal graphene quantum dots with tunable size. J. Am. Chem. Soc. **132**(17), 5944–5945 (2010). doi:10.1021/ja1009376
51. X. Yan, B.S. Li, X. Cui, Q.S. Wei, K. Tajima, L.S. Li, Independent tuning of the band gap and redox potential of graphene quantum dots. J. Phys. Chem. Lett. **2**(10), 1119–1124 (2011). doi:10.1021/jz200450r
52. G. Eda, Y.Y. Lin, C. Mattevi, H. Yamaguchi, H.A. Chen, I.S. Chen, C.W. Chen, M. Chhowalla, Blue photoluminescence from chemically derived graphene oxide. Adv. Mater. **22**(4), 505–509 (2010). doi:10.1002/adma.200901996
53. H. Li, X. He, Z. Kang, H. Huang, Y. Liu, J. Liu, S. Lian, C.H. Tsang, X. Yang, S.T. Lee, Water-soluble fluorescent carbon quantum dots and photocatalyst design. Angew. Chem. Int. Ed. **49**(26), 4430–4434 (2010). doi:10.1002/anie.200906154
54. M.A. Sk, A. Ananthanarayanan, L. Huang, K.H. Lim, P. Chen, Revealing the tunable photoluminescence properties of graphene quantum dots. J. Mater. Chem. C **2**(34), 6954–6960 (2014). doi:10.1039/c4tc01191k
55. D. Pan, J. Zhang, Z. Li, M. Wu, Hydrothermal route for cutting graphene sheets into blue-luminescent graphene quantum dots. Adv. Mater. **22**(6), 734–738 (2010). doi:10.1002/adma.200902825
56. Y. Dong, R. Dai, T. Dong, Y. Chi, G. Chen, Photoluminescence, chemiluminescence and anodic electrochemiluminescence of hydrazide-modified graphene quantum dots. Nanoscale **6**(19), 11240–11245 (2014). doi:10.1039/c4nr02539c
57. P. Anilkumar, L. Cao, J.J. Yu, K.N. Tackett II, P. Wang, M.J. Meziani, Y.P. Sun, Crosslinked carbon dots as ultra-bright fluorescence probes. Small **9**(4), 545–551 (2013). doi:10.1002/smll.201202000
58. S.K. Bhunia, A. Saha, A.R. Maity, S.C. Ray, N.R. Jana, Carbon nanoparticle-based fluorescent bioimaging probes. Sci. Rep. **3**, 1473–1749 (2013). doi:10.1038/srep01473
59. C. Liu, P. Zhang, X. Zhai, F. Tian, W. Li, J. Yang, Y. Liu, H. Wang, W. Wang, W. Liu, Nano-carrier for gene delivery and bioimaging based on carbon dots with PEI-passivation enhanced fluorescence. Biomaterials **33**(13), 3604–3613 (2012). doi:10.1016/j.biomaterials.2012.01.052
60. M. Nurunnabi, Z. Khatun, K.M. Huh, S.Y. Park, D.Y. Lee, K.J. Cho, Y.K. Lee, In vivo biodistribution and toxicology of carboxylated graphene quantum dots. ACS Nano **7**(8), 6858–6867 (2013). doi:10.1021/nn402043c

61. X.T. Zheng, A. Than, A. Ananthanaraya, D.H. Kim, P. Chen, Graphene quantum dots as universal fluorophores and their use in revealing regulated trafficking of insulin receptors in adipocytes. ACS Nano **7**(7), 6278–6286 (2013). doi:10.1021/Nn4023137
62. H. Zhao, Y. Chang, M. Liu, S. Gao, H. Yu, X. Quan, A universal immunosensing strategy based on regulation of the interaction between graphene and graphene quantum dots. Chem. Commun. **49**(3), 234–236 (2013). doi:10.1039/C2CC35503E
63. Y. Wang, L. Bao, Z. Liu, D.W. Pang, Aptamer biosensor based on fluorescence resonance energy transfer from upconverting phosphors to carbon nanoparticles for thrombin detection in human plasma. Anal. Chem. **83**(21), 8130–8137 (2011). doi:10.1021/ac201631b
64. W. Deng, F. Liu, S. Ge, J. Yu, M. Yan, X. Song, A dual amplification strategy for ultrasensitive electrochemiluminescence immunoassay based on a Pt nanoparticles dotted graphene-carbon nanotubes composite and carbon dots functionalized mesoporous Pt/Fe. Analyst **139**(7), 1713–1720 (2014). doi:10.1039/C3AN02084C
65. Z.-X. Wang, C.-L. Zheng, Q.-L. Li, S.-N. Ding, Electrochemiluminescence of a nanoAg-carbon nanodot composite and its application to detect sulfide ions. Analyst **139** (7), 1751–1755 (2014). doi:10.1039/C3AN02097E
66. S. Yang, J. Liang, S. Luo, C. Liu, Y. Tang, Supersensitive detection of chlorinated phenols by multiple amplification electrochemiluminescence sensing based on carbon quantum dots/graphene. Anal. Chem. **85**(16), 7720–7725 (2013). doi:10.1021/ac400874h
67. P.J. Zhang, Z.J. Xue, D. Luo, W. Yu, Z.H. Guo, T. Wang, Dual-peak electrogenerated chemiluminescence of carbon dots for iron ions detection. Anal. Chem. **86**(12), 5620–5623 (2014). doi:10.1021/Ac5011734
68. M. Zhang, H. Liu, L. Chen, M. Yan, L. Ge, S. Ge, J. Yu, A disposable electrochemiluminescence device for ultrasensitive monitoring of K562 leukemia cells based on aptamers and ZnO@carbon quantum dots. Biosens. Bioelectron. **49**, 79–85 (2013). doi:10.1016/j.bios.2013.05.003
69. Y.Q. Dong, C.Q. Chen, J.P. Lin, N.N. Zhou, Y.W. Chi, G.N. Chen, Electrochemiluminescence emission from carbon quantum dot-sulfite coreactant system. Carbon **56**, 12–17 (2013). doi:10.1016/j.carbon.2012.12.086
70. H. Dai, C. Yang, Y. Tong, G. Xu, X. Ma, Y. Lin, G. Chen, Label-free electrochemiluminescent immunosensor for [small alpha]-fetoprotein: performance of Nafion-carbon nanodots nanocomposite films as antibody carriers. Chem. Commun. **48**(25), 3055–3057 (2012). doi:10.1039/C1CC16571B
71. S. Li, J. Luo, X. Yang, Y. Wan, C. Liu, A novel immunosensor for squamous cell carcinoma antigen determination based on CdTe@Carbon dots nanocomposite electrochemiluminescence resonance energy transfer. Sensor Actuat. B-Chem. **197**, 43–49 (2014). doi:10.1016/j.snb.2014.02.066
72. Y.M. Long, L. Bao, J.Y. Zhao, Z.L. Zhang, D.W. Pang, Revealing carbon nanodots as coreactants of the anodic electrochemiluminescence of Ru(bpy)(3)(2+). Anal. Chem. **86**(15), 7224–7228 (2014). doi:10.1021/ac502405p
73. V. Gupta, N. Chaudhary, R. Srivastava, G.D. Sharma, R. Bhardwaj, S. Chand, Luminscent graphene quantum dots for organic photovoltaic devices. J. Am. Chem. Soc. **133**(26), 9960–9963 (2011). doi:10.1021/ja2036749
74. Y. Li, Y. Zhao, H. Cheng, Y. Hu, G. Shi, L. Dai, L. Qu, Nitrogen-doped graphene quantum dots with oxygen-rich functional groups. J. Am. Chem. Soc. **134**(1), 15–18 (2012). doi:10.1021/ja206030c
75. Y. Zhang, C. Wu, X. Zhou, X. Wu, Y. Yang, H. Wu, S. Guo, J. Zhang, Graphene quantum dots/gold electrode and its application in living cell H_2O_2 detection. Nanoscale **5**(5), 1816–1819 (2013). doi:10.1039/c3nr33954h
76. A. Muthurasu, V. Ganesh, Horseradish Peroxidase Enzyme immobilized graphene quantum dots as electrochemical biosensors. Appl. Biochem. Biotechnol. **174**(3), 945–959 (2014). doi:10.1007/s12010-014-1019-7